

# NUMERICAL ANALYSIS OF WELDING PROCESS FOR DISTORTION PREDICTION OF PIPE STRUCTURES FOR AEROSPACE INDUSTRY

S. RASCHE\*, M. FISCHER\*\*, J. HILDEBRAND\*,  
J. P. BERGMANN\*

*\*Technische Universität Ilmenau, 98693 Ilmenau, Germany*

*\*\*PFW Aerospace GmbH, 67346 Speyer, Germany*

DOI 10.3217/978-3-85125-968-1-16

## ABSTRACT

The preferred joining process for lightweight titanium alloyed pipe structures used in aerospace industry is Tungsten Inert Gas welding. The further development and automation of the currently time-consuming and cost-intensive manual production of titanium bleed-air tubes is addressed in the collaborative research project ASciE. The Production Technology Group at Technische Universität Ilmenau works together with PFW Aerospace GmbH to develop finite element simulation models for the distortion prediction of thin-walled welded pipe structures. In this project the influence of varying welding process parameters and heat source models as well as different clamping conditions and thermal boundary conditions on the welded geometry will be studied numerically. The real geometry of the circumferential welded components is measured by means of an optical 3D measurement system, which is well suited for the evaluation of spatial distortions of structures with high resolution. Therefore, the prediction quality of the numerical model can be validated. This conference contribution presents an example of a butt welded pipe component, the results of 3D measurement and the results of finite element analyses. The challenges that arise for a realistic prediction of the welding distortion of the thin-walled pipe component will be discussed.

Keywords: Welding process simulation, TIG welding, distortion prediction, optical 3D scan, thin-walled titanium alloyed pipe structures

## INTRODUCTION

Lightweight structures made of titanium alloys are essential in aircraft construction due to the outstanding properties (low density, high strength, corrosion resistant) of this material. The preferred joining process of the titanium alloy components is Tungsten Inert Gas (TIG) welding. The further development and automation of the currently time-consuming and cost-intensive manual production of titanium bleed-air tubes is addressed in the new research project ASciE (20W1903B), which is funded by German Federal Ministry for Economic Affairs and Climate Action in the framework of Luftfahrtforschungsprogramm

des Bundes (LuFo). The Production Technology Group at Technische Universität Ilmenau works together with PFW Aerospace GmbH to develop finite element simulation models for the distortion prediction of thin-walled welded pipe structures.

High quality demands must be met in the production of the weld seams. The wall thickness of the investigated components ranges between 0.4 mm and 1.6 mm and the tube diameter is about one hundred times the wall thickness. The weld seams are designed as butt joints with an I-seam and technical zero gap. The width of the melting zone is five to ten times the wall thickness. Therefore, it should be obvious that the distortion of the tubes to be welded have to be within a very small range. To capture the actual geometry of the welded components they are measured by means of an optical 3D measurement system (GOM ATOS). By comparing the surfaces of the 3D scanned component and the CAD model, the real spatial deformation can be determined, which can be compared with the predicted deformation from a numerical simulation. This enables the validation of the prediction quality of the numerical model. In this project the influence of varying welding process parameters and heat source models as well as different clamping conditions and thermal boundary conditions will be studied numerically.

This conference contribution shows an example of 3D measurement and finite element simulation of the welding process of a real titanium alloy component and the challenges that arise for numerical analysis.

### DESCRIPTION OF THE COMPONENT AND THE WELDING PROCESS

Fig. 1 shows a photo of the TIG welded titanium alloy component manufactured by PFW Aerospace GmbH with two circumferential seams. The geometry is axially symmetric. The diameter of the tube between the two flanges is 50.8 mm. The wall thickness on both sides of each weld seam is 0.4 mm. The photo shows the measured width of the fusion zone, which varies between 4.0 mm and 4.5 mm, which is more than ten times of the wall thickness. The correct relative positioning of tube and flange is guaranteed by the help of mechanical calibration and mounting tools, which are the experienced know-how of PFW Aerospace GmbH. A multi-part welding insert is mounted before welding and guarantees that the tube diameters of the butt weld are aligned carefully. It has the function of a clamping tool, which fixes the position of the parts to be joined and additionally provides the shielding gas flow at the weld root inside the pipe.

Circumferential TIG welding is performed with argon shielding gas flow on the inside and outside of the pipe. The pipe rotates with horizontal axis of rotation while the welding torch is hold in flat welding position. The filler material is added continuously to the weld bead with a wire feed rate of 70 mm/min. The welding speed is 120 mm/min.

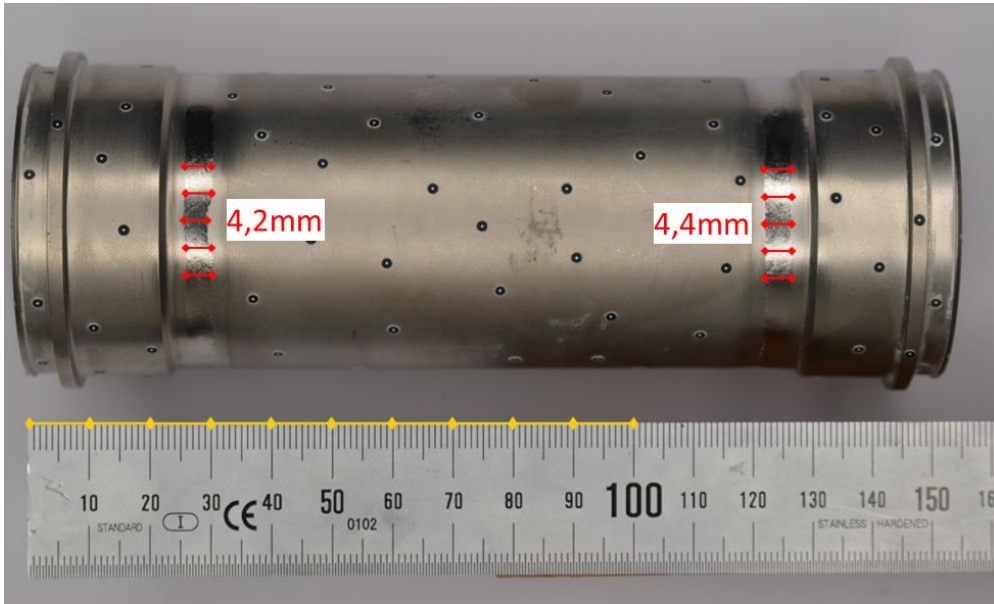


**Fig. 1** Example of a TIG welded titanium alloy component for aerospace industry from PFW Aerospace GmbH. The wall thickness of the pipe component with a diameter of 50.8 mm is only 0.4 mm. The surface is covered with marker points necessary for the 3D scan.

### OPTICAL SCAN OF GEOMETRY

The real geometry of the welded components is measured by means of an optical 3D measurement system, which is well suited for the evaluation of spatial distortions of the structures with high resolution. The industrial metrology 3D scanner GOM ATOS Core 45 (GOM GmbH, Braunschweig, Germany) with a resolution of 0.02 mm was used in our case. A white scanning spray was applied before scanning with the fringe projection technique. The precise fringe patterns are projected onto the surface of the object and are captured by two cameras based on the stereo camera principle. GOM's projection technology works with narrow-band blue light, which means that interfering ambient light can be filtered out during image acquisition.

Small measuring points (0.4 mm) were glued onto the component surface as can be seen in Fig. 1. The measurement points are needed to compute a triangulated surface mesh from a large number of acquired images taken from different spatial directions. The initially computed mesh has 26 million facets. For further processing the file size was reduced to 1.5 million facets using a coarsening and normalization algorithm. The triangulated surface mesh was compared to the CAD model using GOM Inspect software. Fig. 2 shows the calculated deviation of the actual geometry as color-coded plot. Deviation is defined as the shortest distance in the normal direction of the nominal surface of the CAD geometry. A positive deviation means that the actual surface is outside the volume of the CAD model, a negative deviation means that the actual surface is inside the

volume. Fig. 3 shows another enlarged view of the measured deviations. The circular holes are cut-outs at the positions of the marker points.

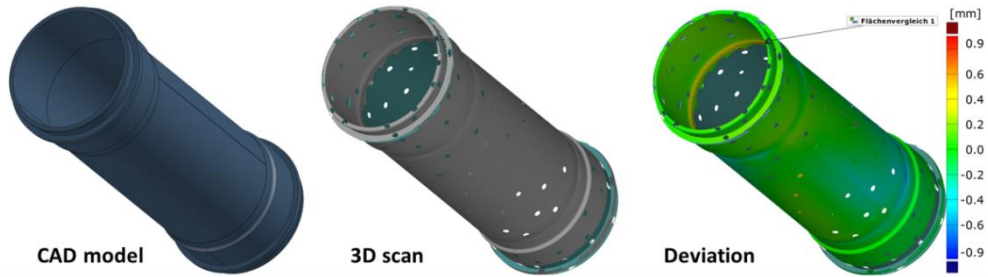


**Fig. 2** Deviation between CAD model and 3D scan of the surface of the welded component

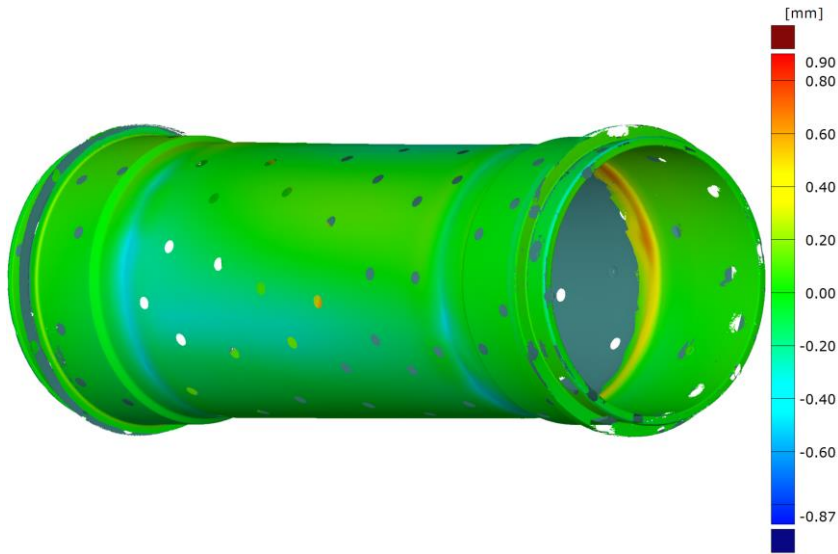


**Fig. 3** Deviation between CAD model and 3D scan of the surface of the welded component

The deviation plots show, that distortions are mainly found in circumferential direction of the two welded seams. The root of both welds has a convex shape with a positive deviation of 0.4 mm to 0.8 mm (yellow to red). The top of the welds have a slightly concave shape with negative deviations up to 0.4 mm (cyan). The other regions in green colour coincide with the CAD surface.

## FINITE ELEMENT MODELING

A finite element model of the welding process has been developed using Simufact Welding 2020. The CAD geometry is imported from STEP files. The material model of



TiAl6V4 with temperature dependent properties is taken from the Simufact Material 2020 database. Transient thermal simulations were performed to calibrate the heat source model before models for the coupled thermo-mechanical simulation were developed. In this paper, only the model for welding simulation of the first of two welds is presented.

#### GEOMETRY AND MESH

The individual parts of the component were imported as STEP files. Simplified geometries of the welding insert and the welding bead were designed and imported as STEP file too. Fig. 4 shows a cross section trough the geometry. The volume of the deposited welding filler material was calculated on the basis of the welding instruction and is  $77 \text{ mm}^3$ .

The deformable parts were meshed with hexahedral solid elements using the Simufact Welding mesher. The overall number of volume elements is 129256. Four element layers of 0.1 mm thickness are used near the weld seam, see Fig. 5. The element edge length in axial and tangential direction is 0.4 mm.

The welding insert, which has the function of a clamping tool, is modelled with rigid surface elements. An interference fit of 0.05 mm is assumed to model the clamping force in an initial simulation step. That means, the inner radius of the pipe will be expanded by 0.025 mm due to the oversize of the welding insert in the contact region.

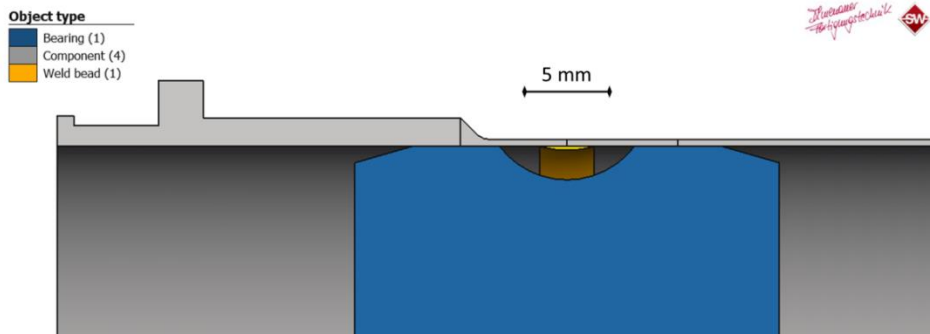


**Fig. 4** Cross section through the axisymmetric geometry of the finite element model

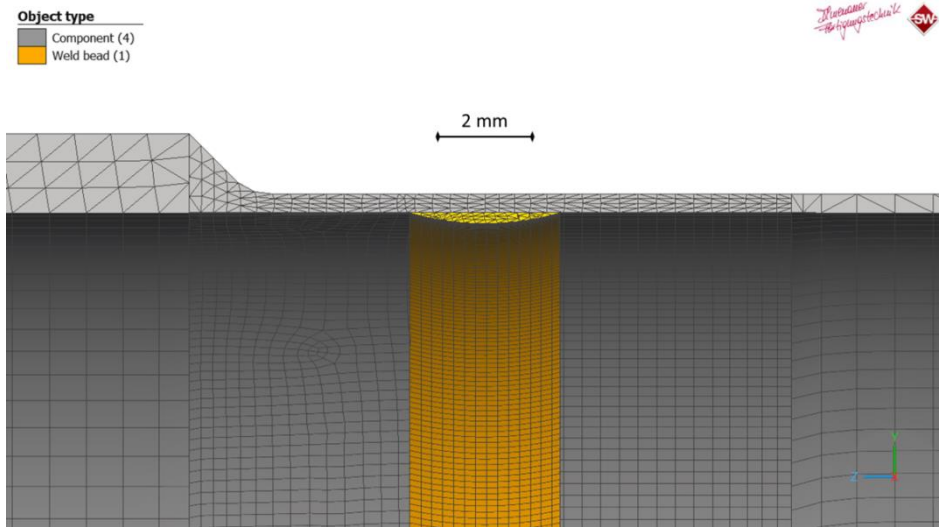


**Fig. 5** Cross section through the mesh of the finite element model near the weld seam

#### MATERIAL MODEL

The material model of TiAl6V4 is taken from the Simufact Material 2020 database. The physical, thermal and mechanical material properties are defined as function of temperature between 20 °C and 1600 °C. Above the last point in the material tables, the material properties are set as constant values. Constants used in the material model are Poisson's ratio, melting enthalpy, solidus temperature and melting temperature, see Table 1. Temperature dependent material properties are defined for thermal conductivity, specific heat capacity, Young's modulus, density, thermal expansion coefficient and yield stress. Their values at room temperature are given in Table 2. The temperature dependent flow curves are shown in the diagram in Fig. 6.

**Table 1** Material constants of TiAl6V4 used in the model

Poisson's ratio	Solidus temperature (°C)	Melting temperature (°C)	Melting enthalpy (J/kg)
0,26	1550	1600	419000

**Table 2** Material parameters of TiAl6V4 at room temperature

Thermal conductivity (W/(m·K))	Specific heat capacity (J/(g·K))	Young's modulus (MPa)	Density (kg/m <sup>3</sup> )	Thermal expansion coefficient (1/K)	Initial yield stress (MPa)
6,0	0,54	115600	4482	8.85·10 <sup>-6</sup>	1170

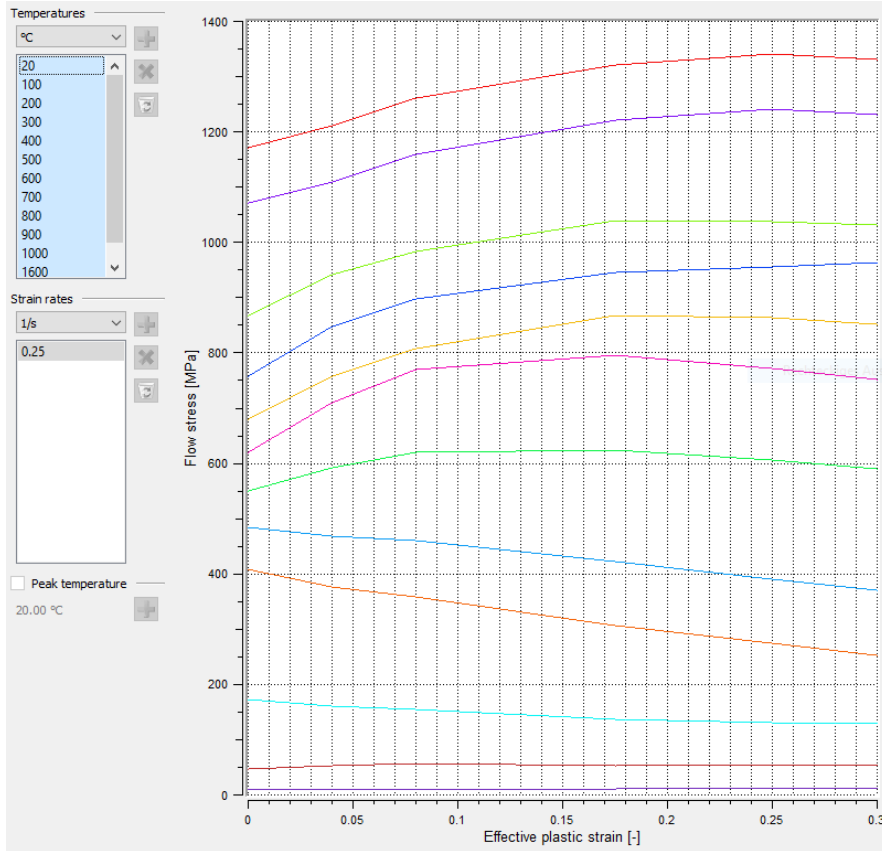


**Fig. 6** Flow curves from 20 °C to 1600 °C for TiAl6V4 from Simufact Material database

### PROCESS PARAMETERS

The welding process parameters were taken from the welding instructions, see Table 3. The efficiency parameter was calibrated together with the heat source model until the simulated width of the fusion zone matches the measured width with an accuracy tolerance of  $\pm 2\%$ .

**Table 3** Welding process parameters used for 0.4 mm wall thickness

Current (A)	Voltage (V)	Welding speed (mm/s)	Energy per length (J/cm)	Efficiency
22	8	2	880	0.8

## HEAT SOURCE MODEL

The heat input  $Q$  is modelled with a volumetric heat source. The double ellipsoid heat source model by Goldak [2] is used as the conventional standard heat source model for arc welding simulations. The spatial distributions of the heat flux density in the front and rear quadrants,  $q_f$  and  $q_r$ , respectively, are defined as

$$q_f(x, y, z) = \frac{6\sqrt{3}f_f Q}{a_f b d \pi \sqrt{\pi}} \exp\left(-3\left(\frac{x^2}{a_f^2} + \frac{y^2}{b^2} + \frac{z^2}{d^2}\right)\right) \quad (1)$$

and

$$q_r(x, y, z) = \frac{6\sqrt{3}f_r Q}{a_r b d \pi \sqrt{\pi}} \exp\left(-3\left(\frac{x^2}{a_r^2} + \frac{y^2}{b^2} + \frac{z^2}{d^2}\right)\right) \quad (2)$$

with a moving local coordinate system  $(x, y, z)$  in the center of the ellipsoid. Five parameters have to be set in Simufact Welding, the half width  $b$ , the depth  $d$ , the front length  $a_f$ , the rear length  $a_r$  and the Gaussian parameter  $M$ , which defines the width of the Gaussian bell curve and is set to 3 by default. The fractions  $f_f$  and  $f_r$  of the heat deposited in the front and rear quadrants must satisfy the condition  $f_f + f_r = 2$  to maintain the total power.

The four geometric parameters represent the size of the weld pool and have to be calibrated. The parameters used in the model are given in Table 4, they were calibrated until the simulated width of the fusion zone matches the measured width with an accuracy tolerance of  $\pm 2\%$ .

**Table 4** Calibrated parameters of the double ellipsoid volume heat source model

Front length $a_f$ (mm)	Rear length $a_r$ (mm)	Half width $b$ (mm)	Depth $d$ (mm)	Gaussian parameter $M$	Heat front fraction $f_f$
1.2	4.0	2.0	1.2	3	0.4615

## RESULTS AND DISCUSSION

### THERMAL SIMULATION

The calibration of the heat source model and the thermal efficiency was performed with a transient thermal model. The following thermal boundary condition settings were used:

- Initial and ambient temperature: 20 °C
- Convective heat transfer coefficient: 20 W/(m<sup>2</sup>·K)
- Contact heat transfer coefficient: 1000 W/(m<sup>2</sup>·K)
- Emission coefficient: 0.6

Fig. 7 shows the simulated width of the weld seam in a plot of peak temperature at a distance of 180° from start of welding. The width varies between 4.2 mm und 4.3 mm with a mean value of 4.25 mm. The simulated width agrees with the median value of the measured width, which varies between 4.0 mm and 4.5 mm.

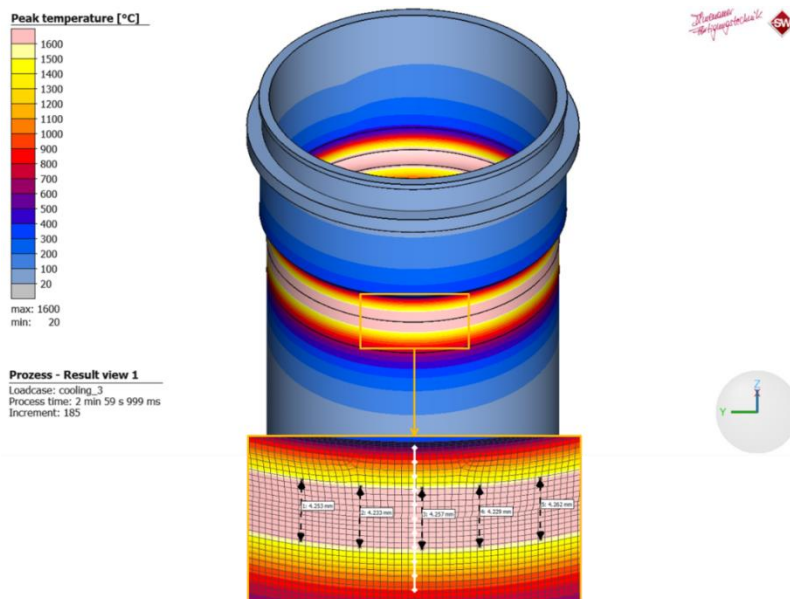


**Fig. 7** Peak temperature plot with measurement of the simulated weld seam width after calibration of the heat source. A 10 mm long evaluation path transverse to the weld seam was drawn into the enlarged image detail.

The corresponding plot of temperature-time history is show in Fig. 8 for eleven equidistant points (distance 1 mm) along a path transverse to the weld seam. Due to the increase in cross section in the flange, the temperature profile is not exactly symmetric with respect to the weld seam.

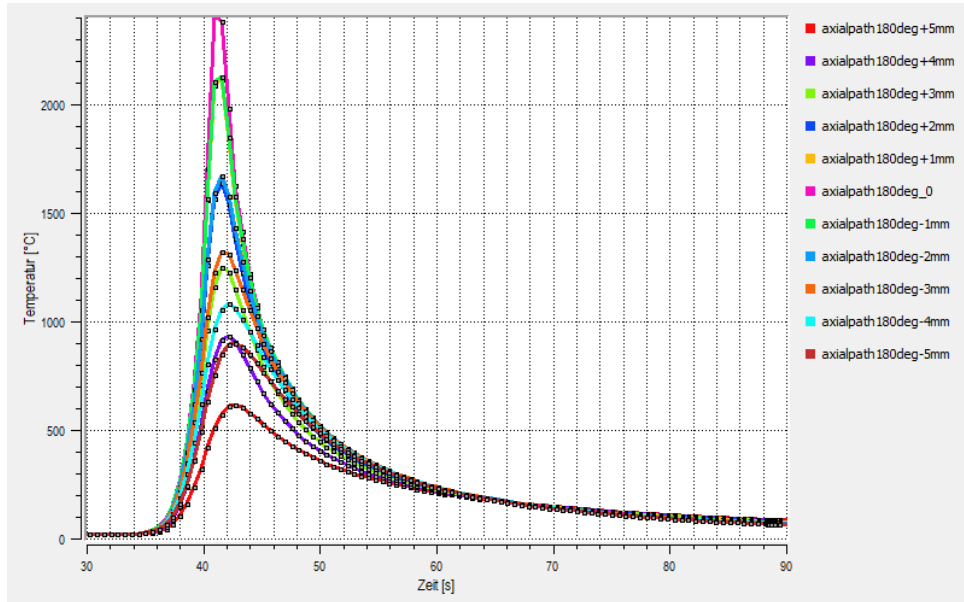
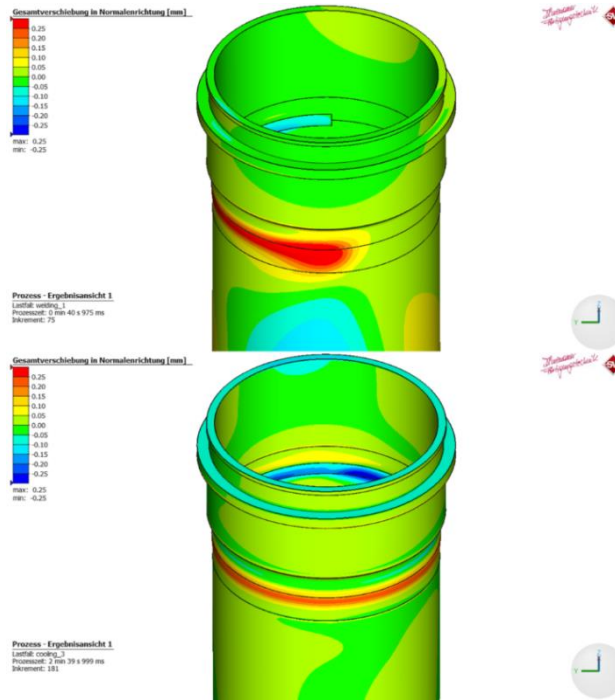


Fig. 8 Computed surface temperatures of points along a path perpendicular to the weld seam

THERMOMECHANICAL SIMULATION

The calculation of deformations and stresses has been performed with a coupled thermo-mechanical finite element analysis using the previously calibrated heat source. The deformations and stresses are influenced not only by the thermal expansion, but also by the clamping forces. Clamping by the welding insert is activated before welding starts and deactivated after cooling. Touching contact is defined between the component and the welding insert with a friction coefficient value of 0.2. Glued contact is defined between different meshes of the same part. Touching contact with glue on peak temperature is defined at the welding seam.

The predicted deformation normal to the surface can be seen in Fig. 9. The upper image shows the deformation of the circumferential weld after 180° have been welded, the lower image shows the deformation at the end of the simulation, when the component has cooled down and the clamping is deactivated. Obviously, the weld seam bulges outwards in this simulation, while the deformation is directed inwards in the 3D scan of the real component. Variations in the heat source and welding process parameters did not fundamentally alter the results. Due to the curvature of the pipe, the heated zone will always bulge outwards when thermal expansion is simulated without additional surface forces.



**Fig. 9** Predicted deformation normal to the surface 180 ° after start of welding (upper picture) and at the end of the simulation (lower picture)

The reason for this incorrect prediction is that compressive forces on the surface of the molten pool are not considered. The formation of the melt pool surface is influenced by gravity, surface tension, arc pressure, evaporation pressure and drop impact pressure [4]. It is known from literature [5], that several welding process parameters influence the arc stagnation pressure significantly. For example, argon shielding gas used for TIG welding increases the arc pressure significantly in comparison with helium [6]. In many cases, these forces can be neglected, if the fusion zone is stabilized by the stiffness of the surrounding material. But in our case, the fusion zone goes through the entire wall thickness and the fusion zone width is at least ten times of the wall thickness. An enhanced model approach, which models this influence in a simplified way, is presented in the next section.

## ENHANCED THERMOMECHANICAL SIMULATION

The measured deformation from the 3D scan and the predicted deformation from the previous model indicate that there is a not negligible compressive force on the weld pool surface that moves with the electric arc and that is directed inward. Considering, that the welding arc acts as a source of force over the molten pool, the arc stagnation pressure is an important variable for the formation of the weld bead geometry and the final quality of the weld seam [5]. From experimental studies of the influence of process gases in TIG

welding [6] is known, that the arc stagnation pressure over radius has the shape of a Gaussian bell curve. We had neither a suitable modelling tool in Simufact Welding 2020 nor the necessary data to model this force directly. Instead, we propose a simple indirect approach to apply a pressure distribution in the desired direction to the weld.

A kinematic constraint is added to the weld zone of the model. A rigid ring shell is inserted to the model with a tight gap to the surface of the pipe. When the deformed pipe surface gets in contact to the shell, a pressure distribution is created, which constraints the further outward expansion. In a first approximation, this model approach can describe the effect of the forces on the surface of the molten zone. The shape and gap distance of such a numerical shaping tool has to be calibrated, of course.

Fig. 10 shows the predicted deformation with a kinematically constrained weld bead formation. An initial contact gap of 0.05 mm is modelled. When the radial displacement of the heat affected zone exceeds 0.05 mm in the previous model, it is constrained in this new model and a surface pressure distribution evolves in the heat affected zone. At the end of the simulation, when the component has cooled down and the clamping is deactivated, the weld seam curves inwards in the same manner as in the 3D scan of the welded geometry.

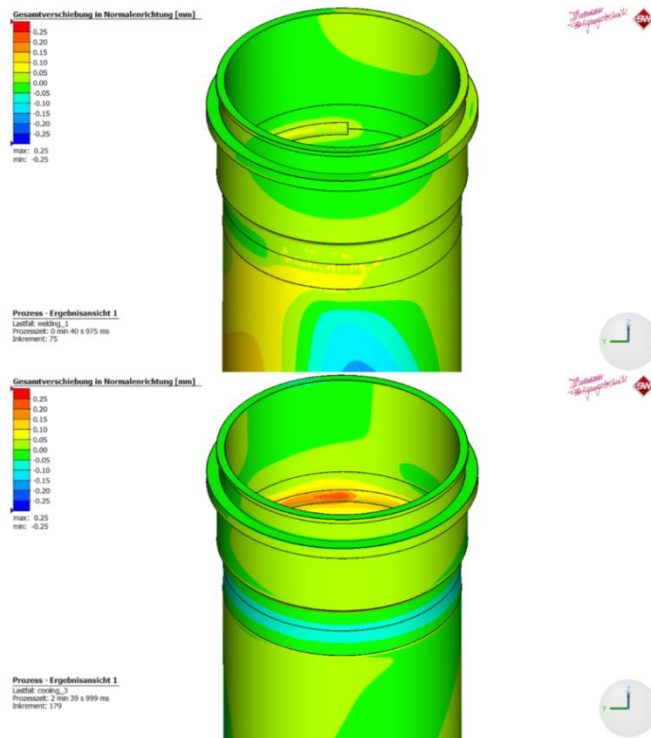


**Fig. 10** Predicted deformation normal to the surface 180 ° after start of welding (upper picture) and at the end of the simulation (lower picture). Simulation results with enhanced model applying a kinematic constraint to the weld zone.



### SUMMARY AND CONCLUSIONS

High quality demands in aircraft industry must be met in the production of the weld seams of lightweight structures. In the same way, numerical models must have a high predictive accuracy if the simulation results are to be used in the design of manufacturing processes. A finite element model for the distortion prediction of a thin-walled TIG-welded titanium alloy pipe component was developed with the purpose of achieving a reliable prediction of the process-induced deformations during welding. The weld seams that were examined are designed as butt joints with an I-seam. The width of the melting zone is ten times the wall thickness.

To capture the actual geometry of the welded components, they were measured by means of an optical 3D measurement system. By comparing the surfaces of the 3D scanned component and the CAD model, it was possible to determine the real spatial deformation, which was compared with the predicted deformation from the finite element analysis. The thermal simulation using a calibrated Goldak heat source provided very accurate results for the size of the fusion zone. The predicted deformations from the thermo-mechanical simulation with the first model unexpectedly gave results that differed significantly from the measured deformations. The simulated weld seam has bulged outwards, while it is slightly curved inwards in reality. The cause was identified in the unconsidered compressive forces on the weld pool exerted by the arc welding process. The thermomechanical model was therefore enhanced with a kinematic constraint approach, which is suited to model these compressive forces indirectly. When material expands radially outward as a result of thermal expansion, an inward directed pressure distribution is generated in the area of the weld zone. By the help of this simple model extension the prediction of the deformations has been substantially improved. With the enhanced model the weld seam curves inwards in the same manner as in the 3D scan of the welded geometry.

From an engineering point of view the presented simplified model approach for considering compressive forces on the weld pool in the finite element analysis leads to satisfying results. However, prior knowledge of the weld bead geometry is necessary, which we obtained from the 3D scan. From a scientific point of view, there is a need for a more physical approach. Like the Goldak heat source for heat input a moving source of distributed mechanical forces acting on the weld pool leading to correct shape of the weld bead surface should be implemented in welding simulation software.

Future work in the research project will focus on the numerical investigation of the influence of modified welding process parameters and mechanical clamping conditions on the distortion of welded pipe structures.

### ACKNOWLEDGEMENTS

The presented research within the collaborative project ASciE (20W1903B) is funded by German Federal Ministry for Economic Affairs and Climate Action in the framework of Luftfahrtforschungsprogramm des Bundes (LuFo). The financial support is gratefully acknowledged.

### References

- [1] E. DOEGE, H. MEYER-NOLKEMPER, I. SAEED: *Fließkurven-Atlas metallischer Werkstoffe*, Carl Hanser Verlag, München Wien, 1986.
- [2] J. GOLDAK, A. CHAKRAVARTI, M. BIBBY: 'A New Finite Element Model for Welding Heat Sources', *Metallurgical Transactions B*, Vol. 15, No. 2, pp. 299-305, 1984.
- [3] J. A. GOLDAK, M. AKHLAGI: *Computational Welding mechanics*, Springer, 2005.
- [4] D. RADAJ: *Schweißprozesssimulation: Grundlagen und Anwendungen*, DVS-Verlag, Düsseldorf, 1999.
- [5] G. DE SIMAS ASQUEL, A. P. S. BITTENCOURT, T. V. DA CUNHA: 'Effect of welding variables on GTAW arc stagnation pressure', *Welding in the World*, Vol. 64, pp. 1149-1160, 2020.
- [6] J. ZÄHR, U. FÜSSEL, M. HERTEL, M. LOHSE, M. SENDE, M. SCHNICK: 'Numerical and experimental studies of the influence of process gases in TIG welding', *Welding in the World*, Vol. 56, pp. 85-92, 2012.